Human Molecular Genetics, 2009, Vol. 18, No. 12 **2099–2114**
doi:10.1093/hmg/ddp133
Advance Access published on March 19, 2009

Gene therapy for retinitis pigmentosa and Leber congenital amaurosis caused by defects in *AIPL1*: effective rescue of mouse models of partial and complete Aipl1 deficiency using AAV2/2 and AAV2/8 vectors

Mei Hong Tan[1], Alexander J. Smith[1], Basil Pawlyk[2], Xiaoyun Xu[2], Xiaoqing Liu[2], James B. Bainbridge[1], Mark Basche[1], Jenny McIntosh[3], Hoai Viet Tran[1], Amit Nathwani[3], Tiansen Li[2,*], and Robin R. Ali[1,*]

[1]Institute of Ophthalmology, NIHR Biomedical research Centre, University College London, London, UK, [2]Berman-Gund Laboratory for the Study of Retinal Degenerations, Harvard Medical School, Massachusetts Eye and Ear Infirmary, Boston, MA, USA and [3]Cancer Research Institute, University College London, London, UK

Received January 5, 2009; Revised and Accepted March 17, 2009

Defects in the photoreceptor-specific gene encoding aryl hydrocarbon receptor-interacting protein-like 1 (*AIPL1*) are clinically heterogeneous and present as Leber Congenital Amaurosis, the severest form of early-onset retinal dystrophy and milder forms of retinal dystrophies such as juvenile retinitis pigmentosa and dominant cone-rod dystrophy. [Perrault, I., Rozet, J.M., Gerber, S., Ghazi, I., Leowski, C., Ducroq, D., Souied, E., Dufier, J.L., Munnich, A. and Kaplan, J. (1999) Leber congenital amaurosis. *Mol. Genet. Metab.*, 68, 200–208.] Although not yet fully elucidated, AIPL1 is likely to function as a specialized chaperone for rod phosphodiesterase (PDE). We evaluate whether AAV-mediated gene replacement therapy is able to improve photoreceptor function and survival in retinal degeneration associated with *AIPL1* defects. We used two mouse models of *AIPL1* deficiency simulating three different rates of photoreceptor degeneration. The *Aipl1* hypomorphic (h/h) mouse has reduced Aipl1 levels and a relatively slow degeneration. Under light acceleration, the rate of degeneration in the *Aipl1* h/h mouse is increased by 2–3-fold. The *Aipl1*−/− mouse has no functional Aipl1 and has a very rapid retinal degeneration. To treat the different rates of degeneration, two pseudotypes of recombinant adeno-associated virus (AAV) exhibiting different transduction kinetics are used for gene transfer. We demonstrate restoration of cellular function and preservation of photoreceptor cells and retinal function in *Aipl1* h/h mice following gene replacement therapy using an AAV2/2 vector and in the light accelerated *Aipl1* h/h model and *Aipl1*−/− mice using an AAV2/8 vector. We have thus established the potential of gene replacement therapy in varying rates of degeneration that reflect the clinical spectrum of disease. This is the first gene replacement study to report long-term rescue of a photoreceptor-specific defect and to demonstrate effective rescue of a rapid photoreceptor degeneration.

INTRODUCTION

Inherited retinal dystrophies are one of the most common causes of blindness in the Western world, affecting approximately 1 in 3000 individuals. To date, there are no effective treatments for this heterogeneous group of conditions that are caused by defects in any one of over 185 different genes, 134 of which have now been identified (www.sph.uth.tmc.edu/Retnet/). A

*To whom correspondence should be addressed. RRA: 11-43 Bath Street, London. Tel: +44 2076086817; Fax: +44 2076086991; Email: r.ali@ucl.ac.uk, or TL: Room 530, Massachusetts Eye and Ear Infirmary, Harvard Medical School, 243 Charles Street, Boston, MA 02114. Tel: (617) 573-3904; Fax: (617) 573-3216; E-mail: tli@meei.harvard.edu.

majority of the defects are in genes that are expressed in either photoreceptors or the retinal pigment epithelium (RPE). There is considerable variation in the severity of these conditions. The most severe are recessive conditions resulting from loss of function; photoreceptor defects tend to result in more severe disease than that caused by RPE defects. This is exemplified by Leber Congenital Amaurosis (LCA), a genetically heterogeneous, autosomal recessive retinal degenerative disease which is the most severe form of inherited retinopathy and the commonest cause of congenital blindness in children accounting for 10–18% of cases (1,2). LCA is characterized by markedly impaired vision or complete blindness and near absence of electrical responses to light within the first year of life.

Over the past two decades, major advances in understanding disease processes in animal models of human retinopathy and the development of efficient retinal gene transfer using either adeno-associated virus (AAV) or lentivirus-based vector systems have led to robust proof of concept studies of gene replacement therapy (3–8). Better outcomes have generally been seen in models of RPE defects (6,9–11) probably due to the fact that gene delivery to RPE cells is more efficient and widespread and more importantly, the photoreceptor cells in these conditions are inherently healthy. The culmination of these developments is the commencement of three human ocular gene therapy trials, treating patients with LCA, caused by mutations in an RPE-specific gene, *RPE65* (12–14). Although the patients involved in these trials were predominantly adults and have established retinal degeneration, the preliminary results suggest some improvement in visual function is possible (12,13), paving the way for additional clinical trials of gene therapy for a variety of inherited retinal degenerations.

In general, gene replacement therapy for photoreceptor-specific defects has not been very effective at slowing severe photoreceptor degeneration characterized by fast progression, such as the *rd1* mice. AAV-based vectors have been shown to be the most efficient vectors for gene transfer to the retina (15,16). A number of AAV serotypes are able to transduce photoreceptors efficiently although AAV2/5 and particularly AAV2/8 appear to be the most efficient (17). The first studies using an AAV2/2 vector in rds mice did not alter rate of retinal degeneration despite the restoration of structure and function—50% of the photoreceptors are still lost by 8 weeks (3,18). More success was achieved in RPGRIP deficient mice following AAV2/2-mediated gene replacement therapy (7). This is possibly due to a requirement for lower levels of transgene expression in RPGRIP deficient mice or because the structural abnormality in *rds* mice was too severe to correct effectively. The speed of disease progression is likely to be important in determining the potential for successful therapy. The window of opportunity in a disease model is created by the balance between time for vector-mediated expression and rate of photoreceptor degeneration. In models of rapid degeneration such as the *rd1* mouse, gene replacement therapy using AAV2/2 vectors is rather unlikely to be successful since most of the photoreceptors are lost before maximal transgene expression can take place. The *rd1* mouse is a well-characterized model of autosomal recessive retinitis pigmentosa and has a very fast retinal degeneration. It is homozygous for a null mutation in the *Pde6b* gene encoding the ß-subunit of rod photoreceptor cGMP phosphodiesterase which results in the loss of function of ß-PDE. Photoreceptor degeneration begins at P10 and is complete by 4 weeks. Despite a number of attempts to treat the *rd1* mice by gene replacement therapy using a variety of vectors (19–22), effective rescue has proved elusive. However, gene replacement therapy has been more effective in *rd10* mice, a hypomorphic *Pde6b* mutant with a missense mutation in exon 13. The mutation causes partial loss of PDE activity and a milder phenotype than the mutation in *rd1* mice. Loss of photoreceptor cells begins at P16 and is complete by P60. Dark rearing slows the degeneration by a further 4 weeks and allows the formation of outer segments that are not normally formed in either *rd10* or *rd1* mice. Pang *et al*. (23) showed it was possible to preserve photoreceptors and retinal function following gene replacement therapy using an AAV2/5 vector. However, animals were dark reared until vector administration at P14 and then dark reared for a further 2 weeks after treatment. They were then exposed to light for 1 week before the effect of treatment was assessed.

The human aryl hydrocarbon receptor-interacting protein-like 1 (*AIPL*1) gene encodes a 384 amino acid protein that incorporates three consecutive tetratricopeptide repeat motifs and shares close structural homology with the FK506-binding protein family of specialized chaperones (24). These features collectively suggest a role for AIPL1 as a molecular chaperone involved in retinal protein folding or cellular translocation (25,26). In patients, *AIPL1* defects are associated with LCA as well as with cone-rod dystrophy and juvenile retinitis pigmentosa (27,28). We have used two mouse models of *AIPL1* deficiency. One model, the *Aipl1*−/− mouse has a targeted disruption of the *Aipl1* gene and produces no Aipl1 (29). The second model, the *Aipl1* h/h mouse, has a targeted disruption of intron 2 that results in reduced levels of *Aipl1* mRNA and a 20–25% reduction in the levels of Aipl1 (30). Pathogenesis of AIPL1-associated retinal degeneration has been linked to cGMP PDE. In parallel to AIPL1 deficiency, all three subunits of the cGMP-PDE holoenzyme (α, ß and γ) were found to be reduced post-transcriptionally in both mouse models, suggesting that AIPL1 may have a role in the post-translational processing of cGMP-PDE. With complete loss of photoreceptors by 3 weeks, the retinal degeneration in the *Aipl1*−/− mouse is even faster than *rd1* mouse. Photoreceptor loss is considerably slower in the *Aipl1* h/h hypomorphic mutant. Retinal degeneration begins after 12 weeks of age and by 6–8 months over half of photoreceptor cells are lost. Constant light exposure further accelerates the degeneration in the *Aipl1* h/h mouse so that photoreceptor cell loss is almost complete by 5 months of age. In these models, normal retinal histology and photoreceptor morphology including outer segments are present at birth and most of photoreceptor cells are lost after the retina has terminally differentiated.

The aim of this study is to develop an effective gene therapy strategy to treat retinal dystrophies due to AIPL1 deficiency. Given the variable severity of disease seen in patients with AIPL1 defects, we assess the efficacy of gene replacement therapy using AAV2/2 and AAV2/8 vectors to treat *Aipl1*−/− and *Aipl1* h/h mice that simulate different rates

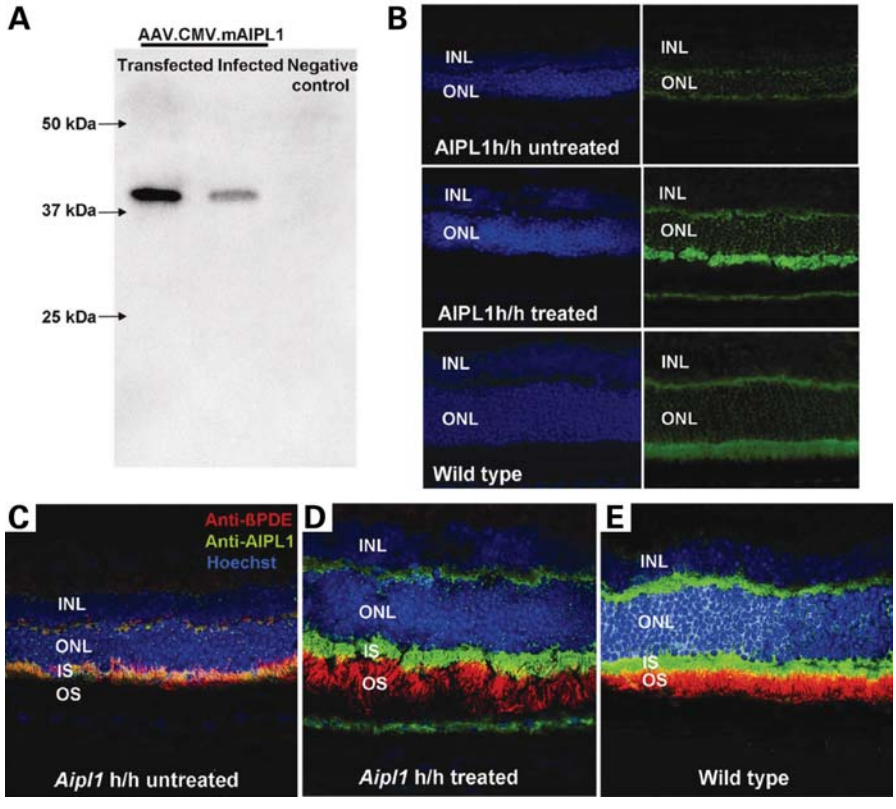

Figure 1. Verification of *Aipl1* expression. (**A**) Western blotting of 293T cells transfected with the plasmid construct and transduced by recombinant vector, AAV2-CMV-*Aipl1* produces a ≈38 kDa protein band corresponding to Aipl1 protein. (**B**) Aipl1 immunofluorescence (green) is reduced in untreated *Aipl1* h/h retina compared with treated retina which shows strong immunofluorescence localized mainly to the inner segments (IS) similar to that seen in wild-type retina. (**C**–**E**) Confocal images of double immunofluorescent microscopy for ß-PDE and Aipl1. In untreated retina, ß-PDE immunofluorescence (red) colocalizes with Aipl1 immunofluorescence (green) in the photoreceptor IS. Following subretinal injection of AAV2-CMV-*Aipl1*, ß-PDE immunofluorescence is translocated to the outer segments (OS) in the treated retina. Hence in treated retina, Aipl1 immunofluorescence in the IS is separate from ß-PDE immunofluorescence in the OS, which is similar to that found in wild-type retina. Cell nuclei are counterstained with Hoechst dye 33342 (blue). INL, inner nuclear layer; ONL, outer nuclear layer.

of retinal degeneration. We assess the effect of gene transfer using light and electron microscopy, immunohistochemistry and by electroretinography. This study is the first to describe long-term rescue of a photoreceptor-specific defect following gene replacement therapy. It also the first to describe the use of an AAV2/8 vector to treat a retinal degeneration and demonstrate effective rescue of a rapid photoreceptor degeneration.

RESULTS

Verification of *Aipl1* transgene expression

The murine *Aipl1* cDNA was PCR amplified from murine retinal cDNA and cloned between into an AAV2 plasmid backbone with a CMV promoter and SV40 polyadenylation site. The plasmid construct pD10/CMV-*Aipl1* and the viral vector AAV2-CMV-*Aipl1* were tested *in vitro* to ensure that they were functional. Transfection using the plasmid construct and transduction using a recombinant AAV serotype 2 vector, AAV2-CMV-*Aipl1*, were performed in 293T cells. Western blot analysis showed a single, appropriate band of 38 kDa (Fig. 1A). We proceeded to test the function of the viral vector in the *Aipl1* h/h mouse model. Messenger RNA was isolated from *Aipl1* h/h retinas 28 weeks after unilateral subretinal injection of AAV2-CMV-*Aipl1* into three animals. Quantitative PCR and paired analysis of the samples showed that the mean relative level of *Aipl1* expression was more than nine times higher than in untreated eyes, although it should be noted that this difference might in part be due to an increased loss of photoreceptor cells in the untreated eyes. The mean relative level in treated eyes at 28 weeks post-injection was approximately half that seen in wild-type animals (data not shown).

AAV-mediated *Aipl1* gene replacement therapy results in increased levels of PDE and restores localization to the outer segment

AAV2-CMV-*Aipl1* was injected subretinally into the superior and inferior hemispheres of the right eyes of 4-week-old *Aipl1* h/h animals ($n = 16$), leaving the contralateral left eye untreated to serve as an internal control for inter-animal variation and test-retest variability. As additional controls, a number of *Aipl1* h/h mice ($n = 5$) received subretinal injections of PBS and wild-type C57B/6 ($n = 6$) received subretinal injections of AAV2-CMV-*Aipl1*. Retinas were analysed at 28 weeks after injection (Fig. 1B). In wild-type mice, Aipl1 was

found mainly in photoreceptor inner segments, but some protein was present in the cell body and synaptic spherules. In uninjected or mock (PBS)-injected *Aipl1* h/h retinas, Aipl1 immunofluorescence was much reduced and there was marked thinning of the outer and inner nuclear layers and disruption of the retinal architecture. Following injection of AAV2-CMV-*Aipl1*, there was a substantial increase in Aipl1 immunofluorescence in appropriate cellular locations. Immunofluorescence was also seen in the RPE layer because AAV2 transduces both photoreceptor cells and RPE and a ubiquitous promoter was used to drive transgene expression.

Since it had previously been suggested that Aipl1 affected rod phosphodiesterase (PDE) levels (29,30), we investigated the effect of rAAV-mediated *Aipl1* gene replacement on rod PDE expression and localization in photoreceptors 28 weeks after vector administration (Fig. 1C–E). Confocal imaging of Aipl1 and β-PDE immunofluorescence in untreated *Aipl1* h/h retinas revealed not only reduced Aipl1 immunofluorescence but also reduced levels of β-PDE which was localized to the inner segments rather than outer segments (Fig. 1C). In eyes that received subretinal AAV2-CMV-*Aipl1*, substantially increased Aipl1 immunofluorescence was accompanied by increased immunofluorescence for ß-PDE. More interestingly, a shift in the subcellular localization of β-PDE was seen in treated retinas; ß-PDE immunostaining was restored to the outer segments of photoreceptors (Fig. 1D). The relative amount and localization of Aipl1 and PDE in treated eyes were similar to that seen in wild-type sections (Fig. 1E). These results indicated that not only the amount of PDE but also its subcellular localization is dependent on Aipl1.

Maintenance of photoreceptor function in *Aipl1* h/h mice following AAV-mediated gene replacement therapy

To evaluate the effect of AAV-mediated *Aipl1* expression on retinal function, dark-adapted, scotopic ERG recordings were obtained from 16 *Aipl1* h/h animals at regular intervals following subretinal injection of AAV2-CMV-*Aipl1* when the animals were 4 weeks old. ERGs were recorded simultaneously from the treated and untreated eyes of each animal. Representative ERG recordings from a single *Aipl1* h/h mouse at 20 weeks post-injection (Fig. 2A) and ERG waveforms at 28 weeks post-injection (Fig.2B) showed that ERG amplitudes in the treated eye were substantially higher compared with the untreated fellow eye. Oscillatory potentials, which represent post-synaptic neuronal activity in the inner retina, were more obvious in the treated eye, but were reduced in the untreated eye. A series of ERG recordings obtained from the treated and untreated eyes of another *Aipl1* h/h animal at various follow-up time points following subretinal injection of AAV2-CMV-*Aipl1* is shown in Figure 2C. Over the 28 week period, the untreated eye showed a steady decline in a-wave and b-wave amplitude, whereas the treated eye showed stabilization of amplitude and waveform with differences apparent from 12 weeks post-injection onwards (Fig. 2C). At 28 weeks, the ERG response from the untreated eye was almost flat, whereas the treated eye maintained a substantial ERG response, indicating preservation of photoreceptor function.

At each time point assessed, there was considerable variation in the ERG amplitudes in the untreated eyes of individual *Aipl1* h/h mice, indicating inter-animal variation in the rate of photoreceptor cell degeneration in this model (data not shown). Furthermore, the ERG results of the same cohorts of animals vary substantially between recording sessions, suggesting high inter-session variability. In view of this variation, paired *t*-tests were used to analyse the mean b-wave and a-wave amplitudes between treated and untreated eyes at the various time points from 4 to 28 weeks (Fig. 2D and E). Both the b-wave and a-wave amplitudes were significantly higher in the treated compared with the untreated eyes at 20, 24 and 28 weeks post-injection ($P \leq 0.05$). There was an initial increase in ERG amplitudes from birth until adulthood (8 weeks) that reflected normal development in mice. Four weeks after vector administration, there was a reduction in b-wave amplitudes in treated eyes that was probably due to injection-related trauma. However, from 20 weeks post-injection onwards, b-wave amplitudes were significantly higher in treated compared with untreated eyes ($P \leq 0.05$), a difference which remained consistent up to the final time point of 28 weeks post-injection. The mean b-wave amplitude in treated eyes ($n = 15$; mean $= 295.3 \pm 13.6$ μV) at 20 weeks post-injection was ∼20% higher that in untreated eyes ($n = 15$, mean $= 243.6 \pm 15.6$ μV). Analysis of mean a-wave amplitudes similarly showed that treated eyes maintained higher amplitudes compared with untreated eyes, this difference was statistically significant ($P \leq 0.05$) from 20 weeks post-injection onwards up to the final time point of 28 weeks post-injection (Fig. 2E). At 20 weeks post-injection, the mean a-wave amplitude in treated eyes ($n = 15$; mean $= 109.6 \pm 20.4$ μV) was ∼38% higher than that in untreated eyes ($n = 15$; mean $= 79.2 \pm 33.8$ μV).

In the group of PBS-injected animals, no significant differences were seen in the b-wave amplitudes between injected and uninjected eyes (Supplementary Material, Fig. S1). No significant differences were found in the b-wave amplitudes in treated and untreated eyes of wild-type C57B/6 mice which received a unilateral subretinal injection of AAV2-CMV-*Aipl1*, indicating that over expression of Aipl1 in photoreceptors and RPE did not affect retinal function (Supplementary Material, Fig. S2A).

AAV-mediated gene replacement therapy increases photoreceptor survival in *Aipl1* h/h mice

The effects of AAV-mediated *Aipl1* expression in the same group of *Aipl1* h/h mice were evaluated by assessing the retinal morphology. Semi-thin sections of treated and untreated *Aipl1* h/h retinas were taken at 52 weeks after unilateral injection of AAV2-CMV-*Aipl1*. Treated eyes had received double subretinal injections of the therapeutic vector in the superior and inferior hemisphere of the eye. Prior to embedding, the eyes were orientated so that sections would be sagittally orientated to show the superior and inferior treated areas of the retina. In treated eyes, the retina had considerably more photoreceptor cell nuclei and the photoreceptor outer segments were longer and more densely packed (Fig. 3A). The preservation of photoreceptor cells was evident throughout the treated retina as seen by the preser-

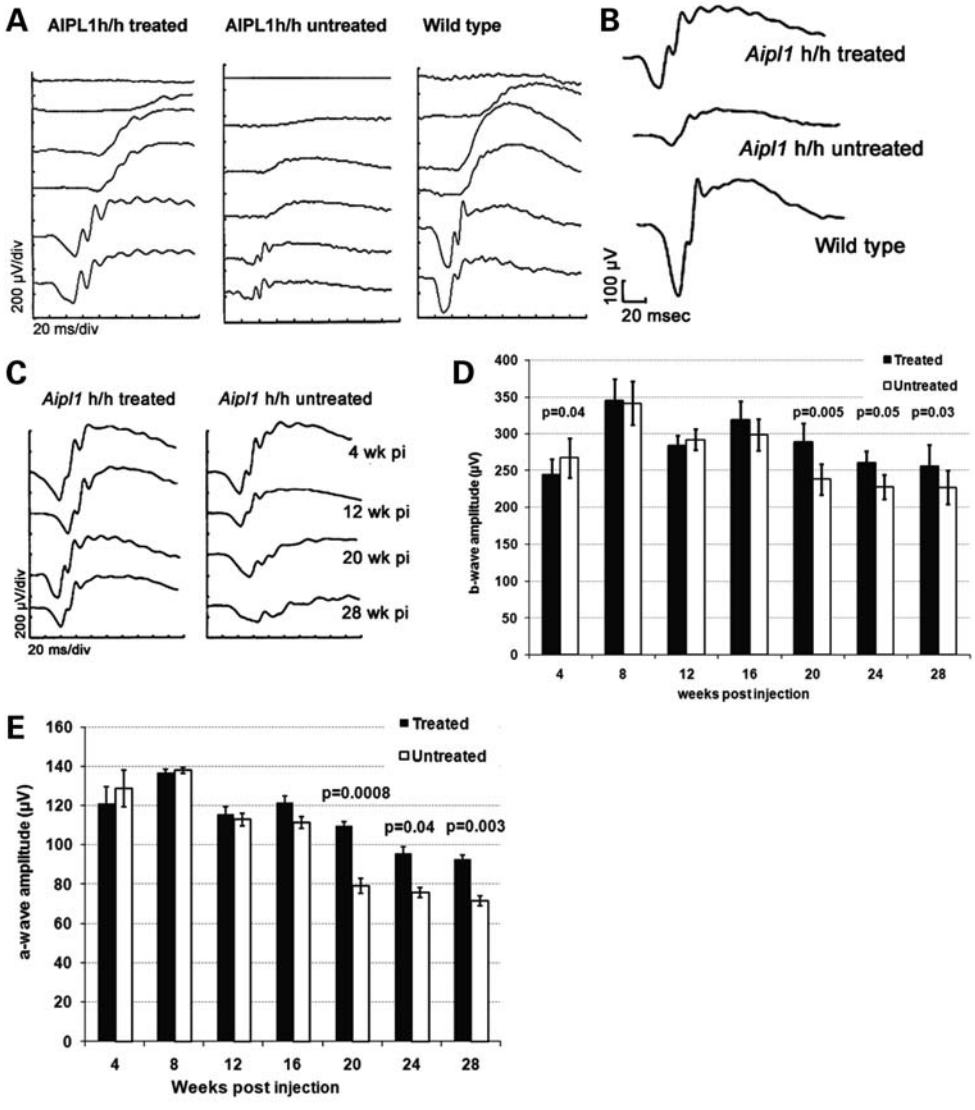

Figure 2. Functional rescue assessed by ERG analysis following subretinal injection of AAV2-CMV-*Aipl1*. (**A**) ERG intensity series at 20 weeks following treatment. ERG traces shown in each chart were recorded at intensities of 0.1, 1, 10, 100, 1000 and 3000 mcds/m^2. The treated eye maintains substantially larger amplitudes and oscillatory potentials while in the untreated eye, there is loss of amplitude even at higher flash intensities. (**B**) Representative ERG waveforms at 28 weeks post-injection from treated and untreated *Aipl1* h/h eyes. A wild-type waveform is shown for comparison. The treated eye shows a discernible a-wave and a higher b-wave compared with the untreated eye. (**C**) A time course series of ERG recordings at the light intensity of 1000 mcds/m^2 from a single *Aipl1* h/h mouse taken at the various time points is shown. ERG amplitudes from the untreated eye diminish with time, whereas ERG responses are maintained in the treated eye. (**D**) Mean ERG b-wave amplitudes at flash intensity of 1000 mcds/m^2 from treated eyes were significantly higher than untreated eyes from 20 weeks post-injection onwards ($P \leq 0.05$). (**E**) Mean ERG a-wave amplitudes at flash intensity of 1000 mcds/m^2 from treated and untreated eyes show that the differences were statistically significant from 20 weeks post-injection onwards ($P \leq 0.05$). Error bars, $\pm$SEM.

vation of the outer nuclear layer around the whole of the sagittal section. Untreated retinas showed substantial loss of photoreceptor cell nuclei and outer segments and this was also seen as a thinning of the outer nuclear layer throughout the sagittal section of the eye (Fig. 3A). Ultrastructurally, differences were seen in morphology of photoreceptor outer segments. The number of photoreceptor outer segments (OS) in untreated *Aipl1* h/h retina was substantially reduced, markedly shortened and disorganized. The OS disk membranes were also disorganized and less tightly packed and there was loss of the normal laminar arrangement (Fig. 3B). Vacuolar inclusions containing debris material was present in the inner segments of the retina (Fig. 3C). The contact between the RPE and photoreceptor OS was also abnormal and reduced. Intervening vacuoles could also be seen between OS tips and the RPE. In contrast, in treated *Aipl1* h/h retina, photoreceptor OS were elongated and the membranous OS disks had a regular and densely packed arrangement (Fig. 3D), which was similar to that seen in wild-type mice (Fig. 3E). The photoreceptor OS in treated retina maintained close contact with the RPE and showed normal interdigitation with the microvilli of the RPE (Fig. 3F).

Morphometric analysis of treated and untreated eyes of *Aipl1* h/h mice at 28 weeks post-injection (Fig. 3G) showed that the mean number of photoreceptor cell nuclei in treated eyes ($n = 7$) was found to be 41% higher than in the untreated eyes (mean photoreceptor cell count in treated

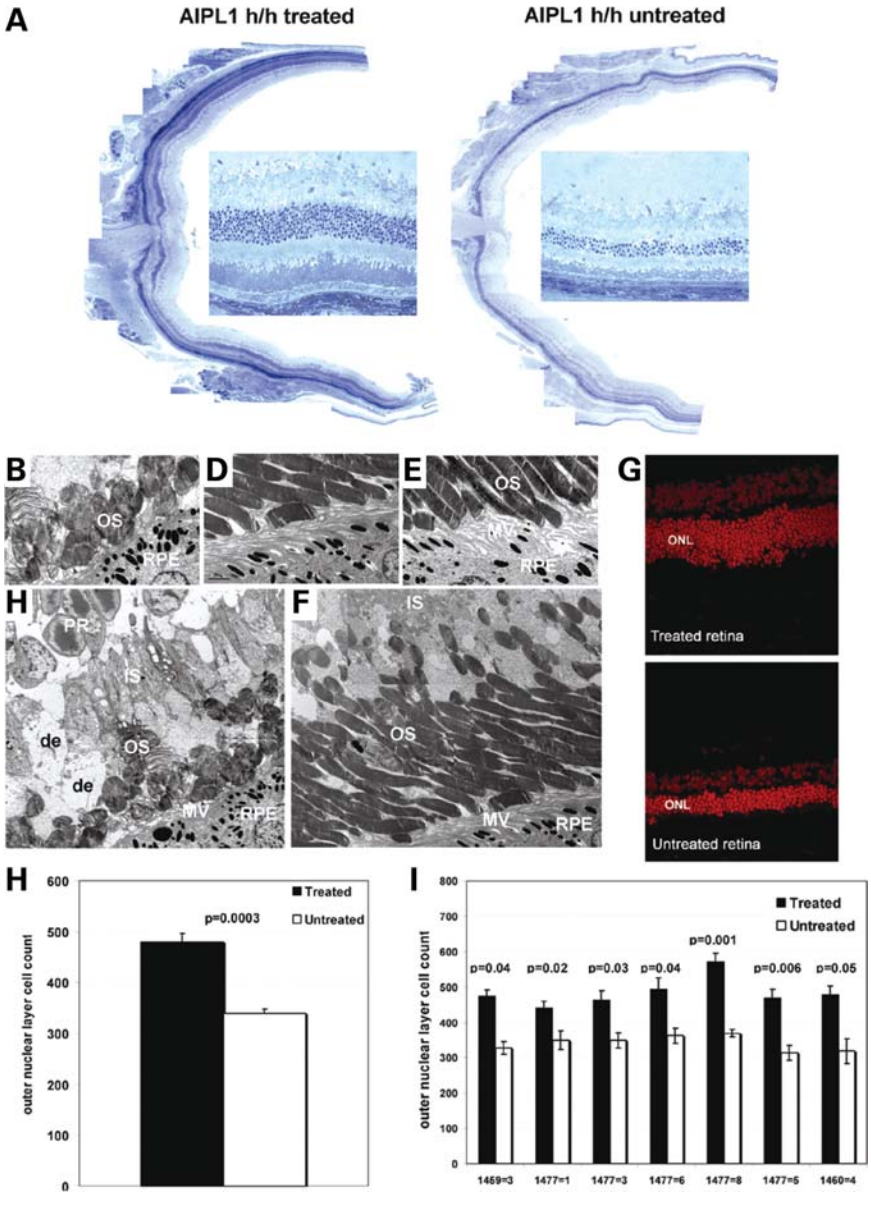

Figure 3. Morphologic analysis of treated and untreated *Aipl1* h/h retina. (**A**) Semithin light micrographs of treated and untreated *Aipl1* h/h retina 52 weeks after injection with AAV-CMV- *Aipl1*. Higher magnification images from the retinas are shown in the centre. The outer nuclear layer (ONL) in the treated retina is substantially thicker and the photoreceptor outer segments (OS) are longer and more densely packed, whereas in the untreated retina, there is loss of outer nuclear layer and outer segments. The sagittal sections show that the preservation of photoreceptors is uniformly present throughout the superior and inferior hemispheres of the treated eye which were the sites of the injections. (**B**–**F**) Electron microscopy (EM) of the same tissue samples. Outer segments in untreated retina are markedly shortened and contain disorganized disks which form whorls instead of stacks (B). There are very few outer segments and multiple debris-filled vacuoles (de) in the retina (C). The treated retina (D) shows long outer segments (OS) with well-organized outer segment disks, resembling those of wild-type retina (E). Outer segments in treated retina are numerous and interdigitate normally with RPE microvilli (MV) (F). IS, inner segments; PR, photoreceptor nuclei. (**G**) Quantitative analysis of the ONL using confocal microscopy shows visibly thicker ONL in treated eyes compared with untreated eyes at 28 weeks post-injection. (**H**) Paired *t*-test showed that the mean ONL cell count of treated eyes was significantly higher than untreated eyes ($P = 0.0003$, $n = 7$). This was consistent in every animal that were assessed (**I**). Error bars, $\pm$SEM.

eyes $= 479.3 \pm 16.6$ versus untreated eyes $= 339.3 \pm 8.2$; $P = 0.0003$) (Fig. 3H). The preservation of photoreceptors in treated eyes was consistent in all of the seven animals assessed, with a significantly greater photoreceptor nuclei count in the treated eye compared with the fellow untreated eye ($P < 0.05$) (Fig. 3I).

The outer nuclear layer was quantified in five wild-type C57B/6 mice that received unilateral subretinal injection of AAV2-CMV-Aipl1 using the same method. Supplementary Material, figure S2B shows confocal images of an injected and uninjected eye from a single wild-type animal. Paired *t*-test showed no significant differences between the mean photoreceptor cell count of wild-type eyes that received subretinal injection of AAV2-CMV-Aipl1 and uninjected eyes (Supplementary Material, Fig. S2C), indicating that there was no detrimental effects on histology or photoreceptor survival.

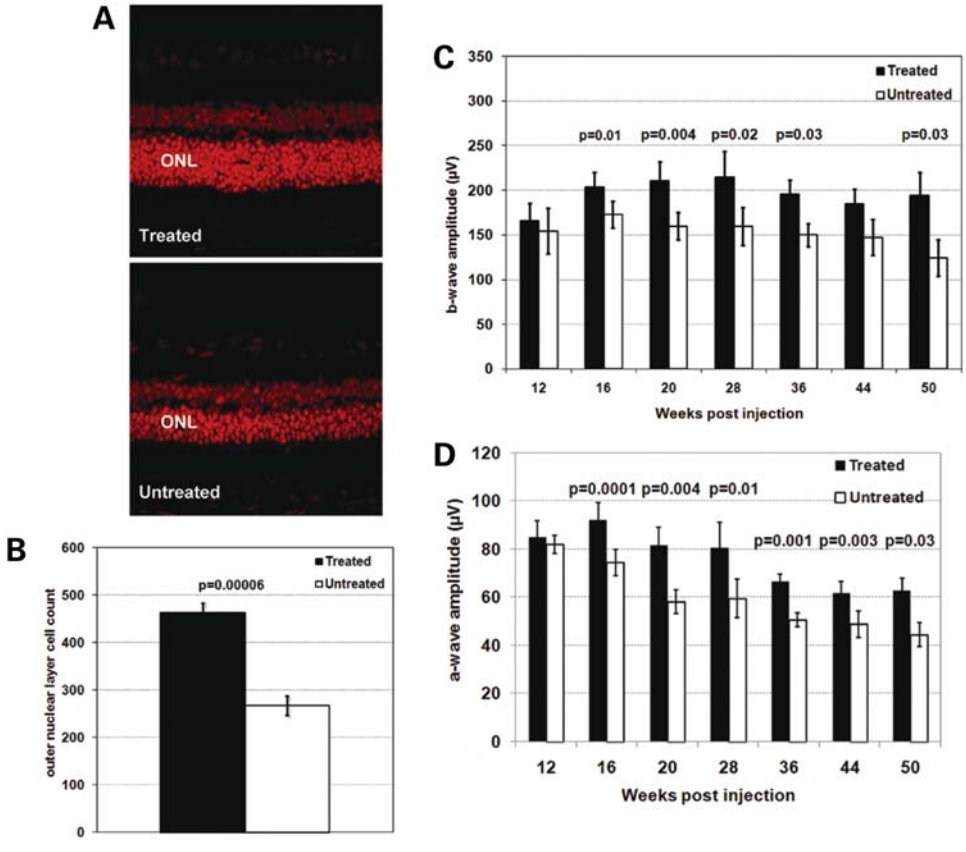

Figure 4. Photoreceptor cell rescue by AAV2/2-mediated expression of human *AIPL1* in *Aipl1* h/h retina. (**A**) Confocal microscopy at 40 weeks post-injection showed visibly thicker outer nuclear layer (ONL) in treated eyes compared with untreated eyes. (**B**) Mean ONL cell counts in treated eyes were significantly higher than untreated eyes ($P = 0.00006$). (**C**) Statistical analysis using paired *t*-test showed that ERG b-wave amplitudes in treated eyes were significantly higher compared with untreated eyes at time points of 16, 20, 28, 36 and 50 weeks post-injection ($P < 0.05$). (**D**) AAV-CMV-*AIPL1* treated eyes showed significantly higher a-wave amplitudes than untreated eyes between 16 and 50 weeks post-injection ($P < 0.05$). Error bars, $\pm$SEM.

AAV-mediated gene replacement therapy using a human cDNA results in effective treatment of *Aipl1* h/h mice

In order to evaluate a therapeutic construct that might be used in clinical studies, we substituted the mouse *Aipl1* cDNA within the expression cassette with a human *AIPL1* cDNA. *Aipl1* h/h mice ($n = 10$) received subretinal injections of AAV2-CMV-*AIPL1* when they were 4 weeks old and were analysed as before using morphological assessments and ERG recording. Follow up, however, included longer time points, up to 50 weeks post-injection (Fig. 4A–C). Paired analysis of photoreceptor cell counts between treated and untreated eyes showed that treated eyes had significantly higher (73% higher) photoreceptor cell count than untreated eyes at 50 weeks post-injection (mean photoreceptor cell count in treated eyes=463.5 $\pm$ 19.8 versus untreated eyes = 267.4 $\pm$ 13.9, $P = 0.00006$, $n = 6$) (Fig. 4A and B). Treated eyes that received subretinal injection of AAV-CMV-*AIPL1* maintained significantly higher b-wave ERG amplitudes up to 50 weeks post-injection ($P = 0.03$) (Fig. 4C). At the final time point of 50 weeks, the mean b-wave amplitude in treated eyes ($n = 10$, mean = 194.6 $\pm$ 25.2 μV) was 57% higher than the mean b-wave amplitude in untreated eyes ($n = 10$, 123.98 $\pm$ 20.42 μV). AAV-CMV-*AIPL1* treated eyes showed significantly higher a-wave amplitudes than untreated eyes between 16 and 50 weeks post-injection ($P < 0.05$) (Fig. 4D).

AAV2/8 mediated gene replacement therapy using a murine cDNA results in effective rescue of light-accelerated retinal degeneration in *Aipl*1 h/h mice

In order to assess the efficacy of gene replacement therapy in the context of a more rapid degeneration, we accelerated the photoreceptor cell loss in *Aipl1* h/h mice by exposing animals to continuous light. We had previously found that *Aipl1* h/h mice kept under constant light exhibited a much faster course of degeneration (our unpublished observation). To ensure that we obtained more rapid onset of gene expression from the AAV vector, we produced AAV2/8-CMV-*Aipl1* by packaging the therapeutic construct using AAV8 capsid. A group of *Aipl1* h/h mice ($n = 23$) received unilateral subretinal injections of AAV2/8-CMV-*Aipl1* when they were 4 weeks old. The mice were placed under constant illumination 1 week after the subretinal injections. Although the retinal degeneration progressed at a faster rate, photoreceptor rescue was still obtained. When the group of AAV2/8-treated *Aipl1* h/h mice that underwent light acceleration was compared with the AAV2/2-CMV-*Aipl1* treated mice, *Aipl1* h/h mice that did not undergo constant

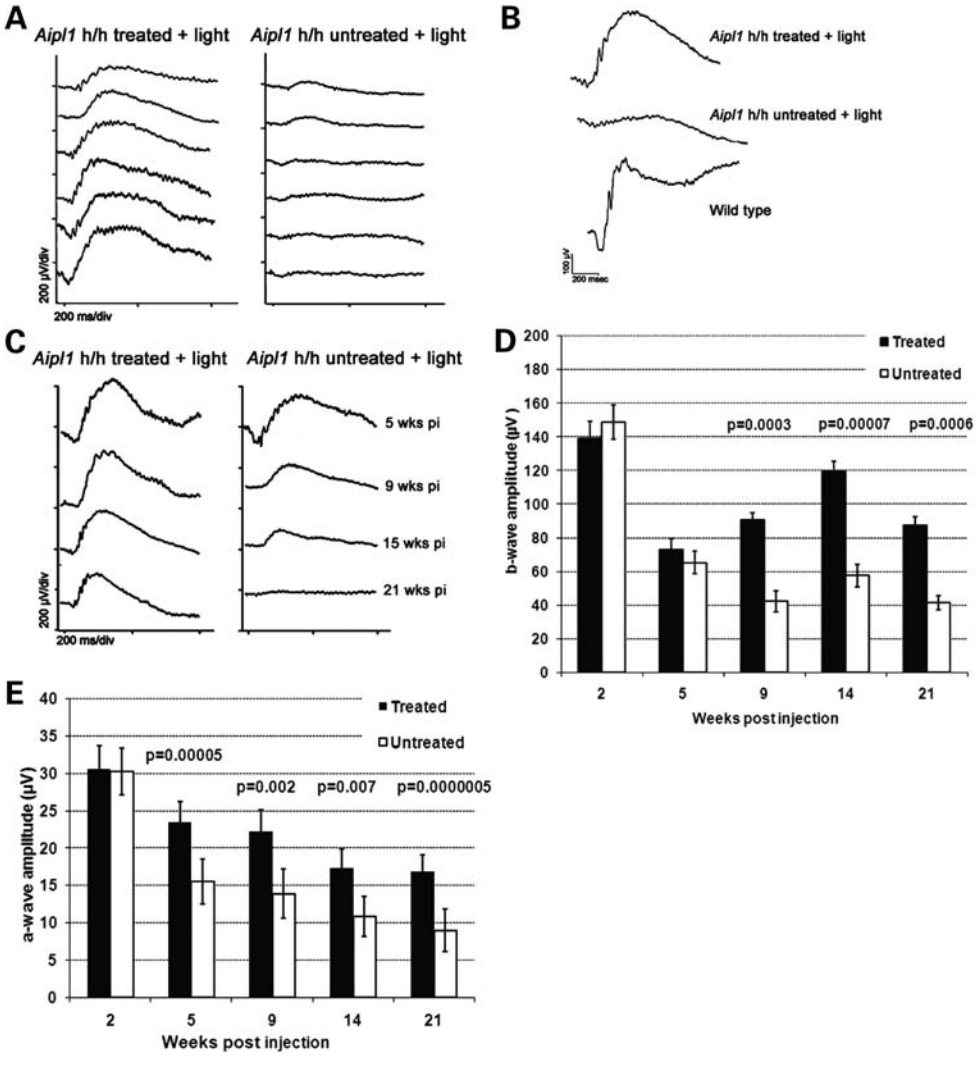

Figure 5. Functional improvement following AAV2/8-mediated *Aipl1* expression. (**A**) ERG intensity series from an *Aipl1* h/h mouse at 21 weeks post-injection under constant light conditions. ERG was recorded flash intensities of 0.1, 1, 10, 100, 1000 and 3000 mcds/m^2. At this time, the treated eye maintains substantial ERG amplitudes whereas the untreated eye shows no discernible ERG response. (**B**) Representative ERG waveforms from a single *Aipl1* h/h mouse at 21 weeks following subretinal injection of AAV2/8-CMV-*Aipl1* and constant light acceleration. (**C**) Representative ERG recordings from a single animal at various time points showing maintenance of ERG amplitudes in treated eye but not in untreated eye. (**D**) Mean ERG b-wave amplitudes at flash intensity of 1000 scotopic mcds/m^2 from treated eyes were significantly higher than untreated eyes from 9 weeks post-injection onwards ($P < 0.05$). Error bars, $\pm$SEM. (**E**) Mean ERG a-wave amplitudes at flash intensity of 1000 scotopic mcds/m^2 from treated eyes were also significantly higher compared with untreated eyes from 5 weeks post-injection onwards ($P < 0.05$). Error bars, $\pm$SEM.

light exposure, larger differences between treated and untreated eyes in terms of functional and morphological outcome measures (Figs 5 and 6) were obtained in the light exposed animals. ERGs were recorded simultaneously from the treated and untreated eyes of each animal. Figure 5A shows a light intensity series at 21 weeks post-injections. At this stage, the

Figure 6. Structural preservation following AAV2/8-mediated *Aipl1* expression. (**A**) Confocal images of the treated and untreated retina from a single *Aipl1* h/h mouse at 21 weeks following subretinal injection of AAV2/8-CMV-*Aipl1*. (**B**) Comparison of the mean ONL cell count ($n = 7$) shows a 123% increase of photoreceptor nuclei in treated eyes compared with untreated eyes ($P = 0.0007$). (**C**) A statistically significant higher ONL count was obtained in the treated eye compared with the untreated eye ($P < 0.005$) in each animal that was assessed. (**D**) Semithin light micrographs of treated and untreated *Aipl1* h/h retina from a single animal 21 weeks after injection with AAV2/8-CMV-*Aipl1*. Preservation of the ONL is evident throughout the treated retina. Higher magnification image shows several rows of photoreceptor nuclei and visible outer segments (OS). The untreated eye has complete loss of ONL and the INL lies adjacent to the RPE layer. (**E**–**H**) EM of the same tissue samples. Photoreceptor outer segments (OS) are present in the treated retina although shortened with some disorganization of the membranous disks (E), and the OS tips appear to invaginate the microvilli (MV) of the RPE. Photoreceptor cells (PR) and OS are numerous with metabolically active inner segments (IS) containing numerous mitochondria (F). The untreated retina shows complete absence of outer segments with debris-filled vacuolar inclusions (de) (G). There is complete loss of photoreceptor cells, only the INL remains lying adjacent to the RPE (H). (**I**) Western blot of retina homogenates from three animals showing increased β-PDE in the treated eye. β-actin was used as loading control. (**J**) Quantification of β-PDE from the three pairs of samples shown as mean $\pm$ SEM and plotted as percentage of the wild-type control. Levels of β-PDE in treated eyes were ~66% of wild-type, whereas untreated eyes had ~9% of wild-type levels ($P = 0.02$ treated versus untreated).

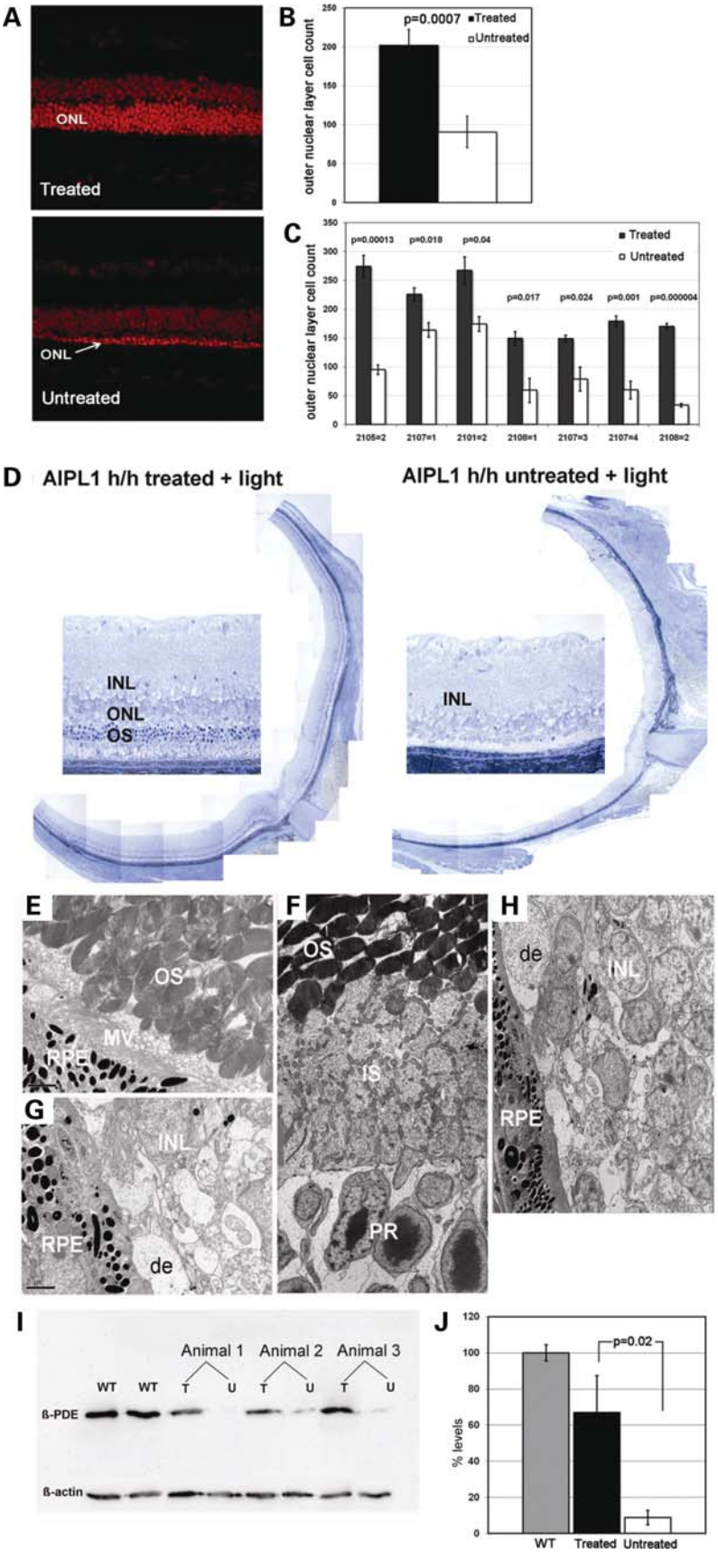

treated eye maintains substantial ERG amplitudes and shows increasing responses elicited by the increasing light stimuli, while ERG responses are lost in the untreated eye. Normally shaped waveforms, similar to that of wild-type mice, were recorded from treated eyes while from untreated eyes, the ERG was virtually undetectable (Fig. 5B). ERGs recorded at the various follow-up time points from a single procedure animal in this group are shown in Figure 5C. Over time, the ERG amplitudes in the untreated eye decreased rapidly and disappeared completely by 21 weeks, while the ERG response in the treated eye was maintained throughout the follow-up period, suggesting that photoreceptor survival was prolonged following treatment with AAV2/8-CMV-*Aipl1*. The apparent improvement in the ERG amplitudes between weeks 5 and 14 was likely to be due to variation occurring between recording sessions. Paired statistical analysis of the mean ERG b-wave amplitudes showed that b-wave amplitudes in treated eyes were significantly higher than untreated eyes up to 21 weeks post-injection (Fig. 5D). At 21 weeks post-injection, the mean b-wave amplitude in treated eyes ($n = 20$; mean $= 87.3 \pm 5.4$ μV) was 110% higher that in untreated eyes ($n = 20$, mean $= 41.5 \pm 4.2$ μV). Analysis of the mean ERG a-waves showed that treated eyes also had significantly higher a-wave amplitudes compared with untreated eyes (Fig. 5E). Statistically significant differences were seen at earlier time points from 5 weeks post-injection onwards up to the last time point of 21 weeks post-injection. At 21 weeks post-injection, mean ERG a-wave in treated eyes was 16.8 ± 2.3 μV ($n = 20$) and in untreated eyes it was 8.9 ± 2.8 μV ($n = 20$).

There were many more photoreceptor cells in treated eyes compared with untreated controls (Fig. 6A). The mean number of photoreceptor nuclei in treated eyes ($n = 7$) was 123% higher than in untreated eyes (mean photoreceptor cell count in treated eyes$=202.1 \pm 20.2$ versus untreated eyes $= 90.64 \pm 23.0$; $P = 0.0007$) at 21 weeks post-injection (Fig. 6B). In each individual animal that was assessed, significant photoreceptor preservation was seen in the treated eye compared with contralateral control (Fig. 6C). In order to assess the extent of photoreceptor preservation, we analysed sagittally orientated semithin retinal sections and found ONL preservation throughout the whole of the eye (Fig. 6D), indicating that the effect of treatment was not localized. Untreated eyes showed complete loss of the ONL by 21 weeks. Electron microscopy of AAV2/8-CMV-*Aipl1* treated eyes showed that although outer segments were present, these were shortened compared with animals which did not undergo light exposure and the membranous disks were less well organized (Fig. 6E). Photoreceptor inner segments appeared to be normal in appearance (Fig. 6F). In untreated eyes, no photoreceptor cells could be seen (Fig. 6G); the inner nuclear layer and bipolar cells were seen to lie adjacent to the RPE, with intervening vacuoles or debris-containing spaces (de) (Fig. 6H).

To investigate the effect of AAV8-mediated *Aipl1* expression on PDE levels, retinal homogenates of treated and untreated eyes were obtained from the AAV2/8-CMV-*Aipl1* injected *Aipl1* h/h mice at 21 weeks after treatment. Western blot analysis of paired retinal homogenates from treated *Aipl1* h/h mice and wild-type controls showed that PDE was present in treated mutant eyes and severely reduced or absent from untreated eyes (Fig. 6I). Quantification of the immunoblots indicated that PDE levels in treated eyes were significantly higher than in untreated eyes ($P = 0.02$). At 21 weeks post-injection with light acceleration, the mean level of PDE in treated eyes was 65% of wild-type levels while in untreated eyes, PDE was 10% of wild-type (Fig. 6J). Since treated eyes at this time point contained approximately half the normal number of photoreceptor cells, following *Aipl1* gene replacement therapy, the level of PDE in each cell might be similar to that in wild-type photoreceptors if we adjust for the number of cells.

Effective rescue of *Aipl1*−/− mice following AAV2/8-mediated gene replacement therapy

Since an AAV2/8 vector proved effective for mediating gene replacement therapy in the light accelerated *Aipl1* h/h model, we proceeded to evaluate the efficacy of AAV2/8-CMV-*Aipl1* mediated gene replacement therapy in the *Aipl1*−/− mouse model that had an extremely fast degeneration. A group of *Aipl1*−/− mice ($n = 12$) received unilateral subretinal injections of AAV8-CMV-*Aipl1*. Because of the early onset of the degeneration, we treated animals when they were 12 days old (P12). Assessments of retinal function and immunohistochemistry were performed 16 days post-injection when the mice were 28 days old (Fig. 7). In untreated *Aipl1*−/− *mice*, the ONL was completely absent, but in treated mice we observed a thick ONL with inner segments containing Aipl1 and outer segments containing PDE. In untreated eyes, no Aipl1 or PDE immunofluorescence was observed. Semithin sections of retina from 4-week-old mice showed that the treatment resulted in substantial preservation photoreceptor cells with long, densely packed outer segments (Fig. 7B). In contrast, no photoreceptor cells could be seen in untreated eyes. ERG recordings were normally extinguished by P18 in the *Aipl1*−/− mouse. While untreated eyes had flat ERG tracings, treated *Aipl1*−/− eyes exhibited good scotopic and photopic ERG amplitudes 16 days after treatment (Fig. 7C). The difference in mean scotopic ERG b-wave amplitudes between treated and untreated eyes was statistically significant ($P = 0.03$; mean b-wave treated $= 243.5 \pm 67.2$ μV, mean b-wave untreated $= 6.25 \pm 8.9$ μV, $n = 4$). At 6 weeks post-injection, treated eyes maintained significantly higher ERG b-wave amplitude compared with untreated eyes ($P = 0.0006$; mean b-wave treated $= 234.7 \pm 51.1$ μV, mean b-wave untreated $= 25.5 \pm 6.4$ μV, $n = 6$). These findings indicated that early treatment using AAV8-CMV-*Aipl1* was able to significantly improve photoreceptor function and delay retinal degeneration in the *Aipl1*−/− mouse. ERG analysis of *Aipl1*−/− mice injected with AAV2/2 therapeutic vector did not show any evidence of preservation function or photoreceptor rescue (Fig. 7D). These mice were also injected at P12 and neither the treated nor the untreated eyes showed any ERG responses at P28 (16 days post-injection).

DISCUSSION

In this study, we have shown that AIPL1-associated retinal degeneration is amenable to gene replacement therapy. We have demonstrated efficacy in animal models of AIPL1

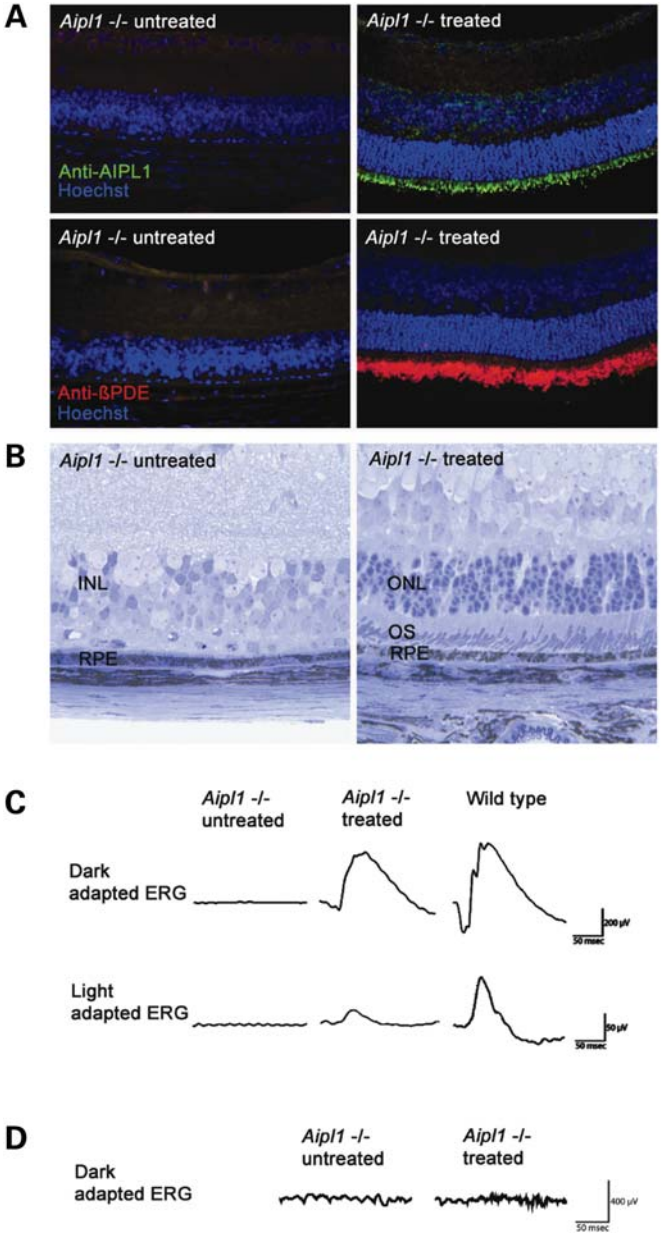

Figure 7. Rescue of the *Aipl1*−/− mouse following subretinal injection of AAV8-CMV-*Aipl1*. (**A**) The untreated eye at 16 days post-injection shows no Aipl1 or β-PDE on immunostaining. Treated eye shows strong murine Aipl1 immunofluorescence (green) in the inner segments and β-PDE immunofluorescence (red) in the outer segments. (**B**) Semithin sections at 19 days post-injection from a procedured *Aipl1*−/− mouse. The ONL is absent in the untreated retina. The treated retina show preservation of photoreceptor outer segments (OS) and six to seven rows of photoreceptor nuclei in the outer nuclear layer (ONL). (**C**) Representative dark and light adapted ERG waveforms from the untreated and treated eyes of single *Aipl1* h/h mouse at 16 days post-injection. The ERG is extinguished in the untreated eye while there is a good b-wave amplitude from the treated eye. An ERG tracing from a wild-type mouse is shown for comparison. (**D**) ERG recordings from *Aipl1*−/− mice injected with the AAV2/2 therapeutic vector did not show any ERG responses from the treated and untreated eyes at 16 days post-injection.

deficiency that exhibit three different rates of degeneration. We demonstrate efficacy first in the hypomorphic *Aipl*1 h/h model and then in increasingly rapid degenerations, specifically the light accelerated *Aipl1* h/h model and the *Aipl*1−/− model. This study demonstrates the effective long-term rescue of a photoreceptor-specific defect and the most effective rescue to date of a rapid retinal degeneration.

In general, gene-based treatments for autosomal recessive retinal dystrophies require not only restoration of function to affected cells but also the prevention of photoreceptor cell death. In this study, we demonstrate that we are able to correct the cellular defect. Following subretinal delivery of *Aipl1* replacement genes packaged in either AAV2 or AAV8 vectors, there is increased production of Aipl1 in photoreceptor inner segments and this led to increased levels of PDE and the restoration of normal PDE translocation from the inner to the outer segments. As a result, retinal degeneration is significantly slowed. We observe improved photoreceptor cell survival, preservation of outer segment morphology and stabilization of retinal function. Both therapeutic constructs, one containing the murine *Aipl1* cDNA and the other containing the human *AIPL1* cDNA are similarly effective. This is not surprising since *AIPL1* is highly conserved between species; there is 96% similarity and 86% identity between the murine and human cDNAs.

AAV-mediated gene replacement therapy results in a significant preservation of photoreceptors and retinal function in *Aipl1* h/h mice 1 year after treatment—the latest time point examined. This is the most sustained rescue of a photoreceptor-specific gene defect reported to date. The most sustained rescue reported previously was following AAV-mediated gene replacement therapy in an *RPGRIP* deficient mouse model, in which photoreceptors were preserved for 5 months (7). Photoreceptors are still present in untreated *Aipl1* h/h mice that are 12 months old and the duration of rescue probably reflects the mild phenotype and slow rate of degeneration. Retinal degeneration is more severe in *Aipl1* h/h mice kept under constant light, with loss of 84% of photoreceptors by 5 months. This can be attributed to a heightened sensitivity of the *Aipl1* h/h mice to light stimuli, as WT mice kept under identical conditions show no light damage at all. Despite the more rapid cell loss, we still observe very significant preservation of photoreceptor cells and retinal function 5 months after gene replacement therapy using an AAV2/8. While rearing animals in continuous light accelerates photoreceptor loss in *Aipl1* h/h mice, even faster retinal degeneration occurs in *Aipl1*−/− mice with all photoreceptors lost by the time animals are 3 weeks old. Following AAV2/8 mediated gene replacement therapy in *Aipl1*−/− mice, we have been able to achieve significant preservation of photoreceptor and retinal function for over 3 months, the last time point tested so far. This represents the most effective rescue to date of a rapid retinal degeneration.

AAV-mediated gene replacement therapy does not completely prevent loss of photoreceptor cells. At 50 weeks, AAV2-CMV-*AIPL1* treated eyes from *Aipl1* h/h mice has on average ∼15% fewer photoreceptor cells than normal wild-type mice, while untreated eyes has ∼50% fewer photoreceptor cells. Although gene replacement therapy in *Aipl1*−/− mice using AAV2/8 is remarkably effective, at 8 weeks after vector administration, treated eyes contain ∼10% fewer photoreceptors than wild-type eyes (data not shown). There may be several reasons why photoreceptor degeneration proceeds despite treatment. First, only two-thirds

of the retina (at most) has been transduced. Secondly, even earlier intervention than postnatal day 12 might be necessary for maximal therapeutic effect. In this regard, it is noted that AAV8 could take 3–4 days to turn on the expression of the therapeutic gene. By then, mice will be over 15 days of age when substantial cell loss is known to have occurred. Thirdly, expression level from the CMV promoter might not have been optimal for *AIPL*1.

In these experiments, we injected a single eye of each animal with therapeutic vector leaving the contralateral uninjected eye to serve as an internal control. Injection of a control vector into the contralateral eye would allow assessment of therapeutic transgene expression in isolation. However, the main aim of this study was to determine the overall therapeutic benefit of subretinal injection of an AAV vector expressing *Aipl1*.

Interestingly, preservation of photoreceptors in *Aipl1* h/h mice is better than might have been expected given the relatively modest difference in ERG amplitudes between treated and untreated eyes. This is most likely due to the peculiar ERG phenotype of the *Aipl1* h/h mice. It has previously been shown that *Aipl1* h/h rods have a higher sensitivity to light compared with normal rod photoreceptor cells, and require fewer photons to elicit a response (30,31). They manifest supranormal ERG when young, presumably because of a larger than normal dark current due to higher free cGMP levels. In this regard, the *Aipl1* h/h mice are reminiscent of rod heterozygotes, which are similarly haploinsufficient for PDE. The restoration of functional AIPL1 in *Aipl1* h/h rods should, therefore, result in correction of this abnormality so that photoresponses become more similar to that of wild-type photoreceptors with a reduction in the altered sensitivity of *Aipl1* h/h rods. Hence, it is likely that the relatively modest difference in ERGs compared with difference in photoreceptor preservation seen after treatment is partly due to a reduction in ERG amplitudes as a result of a reduction in photoreceptor hypersensitivity following gene transfer.

A number of studies have suggested various roles for AIPL1 in the retina. It was originally suggested that AIPL1 may have a role in development as a result of its putative interactions with NUB1 (32), but this is unlikely since both *Aipl1*−/− and *Aipl1* h/h mice have normal retinal architecture prior to the onset of degeneration (29,30). Biochemical studies using a yeast two-hybrid screen suggested that AIPL1 may have a general role in enhancing the protein farnesylation in the retina. Among retinal proteins known to be farnesylated are PDE α-subunit, γ-transducin and rhodopsin kinase. However, this hypothesis does not appear to be supported by the finding that levels of rhodopsin kinase and transducin are unaffected in *Aipl1*−/− mice (29). Further assessment of candidate retinal proteins in the *Aipl1*−/− and *Aipl1* h/h mice suggested that cGMP-PDE is the only protein that is reduced in levels, suggesting that cGMP-PDE is a specific client protein of AIPL1 (29,30) This study confirms that AIPL1 and cGMP-PDE are intricately linked. We find that cGMP-PDE, in particular the β-subunit of PDE is mislocalized to photoreceptor inner segments in untreated *Aipl1* h/h eyes when the animals are examined at 28 weeks following subretinal injection in the other eye. In the contralateral treated eyes of these animals, the β-PDE signal is present in the photoreceptor outer segments suggesting that AIPL1 could indeed be a molecular chaperone ensuring PDE translocation or transport to the outer segments. The fact that photoreceptor cell loss in the *Aipl1* h/h mouse proceeds slowly and outer segments are present for most of the degeneration makes it possible to compare and localize β-PDE expression in the outer segments of treated and untreated eyes. In the *Aipl1*−/− mouse, the retinal degeneration is too rapid for this analysis since most of the photoreceptors cells and outer segments have been lost in the untreated eye by the time AAV8-mediated expression of *Aipl1* commences in the treated eye. Hence, Aipl1 may protect PDE subunits from proteosomal degradation or assist in the assembly or folding of the PDE holoenzyme whereby only properly folded protein is transported to the outer segments. The exact molecular mechanism and relationship between AIPL1 and cGMP-PDE remains to be elucidated. Precise regulation of cGMP synthesis and cGMP-PDE degradation is critical to the health of photoreceptors and mutations which disrupt the balance between the two, result in dysregulation and degeneration of these cells (33). Mutations in the *PDE6B* gene encoding the ß-subunit of cGMP-PDE lead to abnormal increases in cGMP and subsequent photoreceptor death. Mutations in retGC1 impair synthesis of cGMP, leading to a state equivalent to sustained photo-excitation and photoreceptor cell death (33–35). Similarly, one of the most important consequences of mutations in AIPL1 is likely to be the effect on cGMP-PDE levels, leading to photoreceptor dysfunction and rapid retinal degeneration.

This study describes the first use of AAV2/8 to treat a murine model of retinal degeneration. Compared with AAV2/2 and AAV2/5, AAV2/8 is much more efficient at transducing the retina (17) (36). This study evaluates the gene replacement therapy using AAV2/2 and AAV2/8 vectors and finds that the most effective rescue is achieved using AAV2/8. Superior results using this vector may result from its higher transduction efficiency and higher levels of maximal transgene expression. The *Aipl1*−/− mouse has a rapid retinal degeneration that is complete by 3 to 4 weeks of age. Since the onset of AAV2/2 mediated transgene expression occurs between 3 and 4 weeks following subretinal injection, it is not surprising that we do not see any evidence of photoreceptor rescue following treatment of *Aipl1*−/− mice using AAV2/2-CMV-*AIPL1*. The first signs of degeneration in the *Aipl1* h/h mouse are seen at 12 weeks. By injecting AAV2/2 vectors into 4-week-old *Aipl1* h/h mice, AAV2/2-mediated gene expression will be expected to commence by 7 to 8 weeks of age and maximal transgene expression by 16 weeks of age, allowing adequate time for transgene expression before significant photoreceptor degeneration occurs. Constant light exposure accelerates the *Aipl1* h/h retinal degeneration by 2–3-fold so that the ONL is reduced to a single cell layer by 20–21 weeks. For effective treatment of this animal model, a vector with faster transduction kinetics is required. The onset of AAV2/8-mediated gene expression in photoreceptors is known to occur 3–4 days after subretinal delivery and maximal expression by 7 weeks (17). Effective rescue of the accelerated model using an AAV2/8 vector suggests that *Aipl1*−/− mice may be amenable to treatment. To ensure adequate transgene expression before all photoreceptor cells are lost, *Aipl1*−/− mice are treated

when they much younger, 12 days old. The potential benefit of gene transfer has to be balanced against risks of retinal damage in younger mice. At P12, mice have a fully developed retina and have opened their eyes, thus facilitating subretinal injection. AAV2/8-mediated gene expression should occur by P15–16, at which stage there are still surviving photoreceptors. We observe photoreceptor rescue with AAV2/8 but not with titre-matched AAV2/2 in the *Aipl1*−/− mouse which has very rapid and severe photoreceptor degeneration. This suggests that AAV2/8 vector is more efficacious which may be due to its faster transduction kinetics and higher levels of expression in photoreceptor cells, properties which have been previously described (17) (36). However, since a different purification method was used to produce AAV2/8 vector, we cannot exclude the possibility that this might in part be responsible for the higher therapeutic efficacy of this AAV serotype.

In patients, *AIPL1* defects are associated with LCA as well as with cone-rod dystrophy and juvenile retinitis pigmentosa (27,28). The variability in phenotype may be explained by the nature of the mutations. To date, 20 disease-causing mutations in *AIPL1* have been reported (HGMD; www.hgmd.org). Of these, five are likely to lead to complete loss of AIPL1 function; four are nonsense mutations resulting in a severely truncated protein and one affects the splice site in intron 2 leading to a frame shift. The other mutations are missense mutations in the N-terminal or the tetratricopeptide domains and deletions in the C-terminal region. *In vitro* assays have shown that many of these mutations do not lead to the loss of *AIPL1* expression and are unlikely to abolish protein function completely (32,37,38). It is also likely that there are other variants that give rise to altered protein with reduced function. In this study, we have assessed the potential for gene replacement therapy for AIPL1 deficiency, using mouse models with partial or absent function and different rates of retinal degeneration. Efficient rescue of *Aipl1* h/h and *Aipl1*−/− mice suggests that patients with mutations that do not result in a complete loss of AIPL1 function might respond particularly well to gene replacement therapy and that treatment may also be effective in LCA patients with completely absent AILP1 function provided intervention occurs early in life.

MATERIALS AND METHODS

Plasmid constructions and production of recombinant AAV2 and AAV8

The murine *Aipl1* cDNA was PCR amplified from murine retinal cDNA using primers which have been designed to encompass the whole of the coding region. The PCR fragment obtained (1016 bases) was sequenced after cloning into pGem-T (Promega, Madison, WI, USA). The *Aipl1* cDNA was cloned between the CMV promoter and the SV40 polyadenylation site of the construct AAV-CMV-GFP (39) to form the construct pD10/CMV-*Aipl1* (total length 5739 bases). Recombinant AAV2 vector was generated from the murine construct as described (39). The human *AIPL1* cDNA was also PCR amplified from human retinal DNA using primers which covered the whole coding region and included part of the untranslated regions at the 5′- and 3′-ends. The PCR fragment of 1215 bases was cloned into pGem-T (Promega Madison, WI, USA) and checked by sequencing. The *AIPL1* cDNA was inserted into the parental plasmid AAV-CMV-GFP, replacing the GFP gene to generate the human construct pD10/CMV-*AIPL1*. The plasmids were packaged into AAV2 and AAV8 to generate two pseudotyped AAV viral vectors, AAV2-CMV-*AIPL1* and AAV8-CMV-*Aipl1*, as described below.

Recombinant AAV serotype 2 vectors were produced from the constructs encoding murine *Aipl1* and human *AIPL1* by a method described previously, which uses a replicating amplicon pHAV7.3 containing the *rep* and *cap* genes, and PS1 helper virus (39). The constructs described above and the pHAV7.3 amplicon were used to transfect BHK cells by incubation with a mixture of three components, peptide6 ((K16)GACRRETAWACG) (an integrin-targeting peptide), plasmid DNA and lipofectin (Invitrogen Ltd., Paisley, UK) in OptiMEM. BHK cells were transfected with the mixture containing a total of 60 μg of plasmid DNA for 4 h, and followed by incubation with DISC-HSV (PS-1) as helper virus (39). After 36 h, at completion of the lytic cycle, the cells were collected, centrifuged and lysed by repeated freeze thawing. AAV2/2 was purified using a heparin column. Recombinant AAV serotype 8 vector was produced through a triple transient transfection method as described previously (40). The plasmid construct, AAV8 packaging plasmid and helper plasmid were mixed with 2.5 M calcium chloride and 2X HEPES buffered saline to form transfection complexes which was then added to 293T cells and left for 72 h. The cells were harvested, concentrated and lysed to release the vector. The vector was purified by ion exchange chromatography. Both of the AAV2/2 and AAV2/8 virus preparations were concentrated using Centricon 10 columns (Millipore, Bedford, MA, USA), washed in PBS and concentrated to a volume of 100–150 μl. Viral particle titres were determined by comparative dot-blot DNA prepared from purified viral stocks and defined plasmid controls. Purified vector concentrations used for all experiments were $1–2 \times 10^{12}$ viral particles/ml.

Subretinal injection

Subretinal injections were performed on *Aipl1* h/h mice at 4 weeks after birth. Surgery was performed under direct ophthalmoscopic control through an operating microscope. The tip of a 1.5 cm, 34-gauge hypodermic needle (Hamilton, Switzerland) was inserted tangentially through the sclera of the mouse eye, creating a self-sealing scleral tunnel wound. The needle tip was brought into focus in the subretinal space and 1.5 μl viral suspension was injected into the subretinal space to create a bullous retinal detachment around the injection sites. Two subretinal injections were performed for each mouse eye, one in the superior hemisphere and one in the inferior hemisphere. *Aipl1*−/− mice were injected at P12–13 days of age.

In vitro assessment of plasmid construct and viral vector and quantitative PCR

Functional assessment of the construct pD10/CMV-*Aipl1* and expression of *Aipl1* by AAV-CMV-*Aipl1* was assessed

in vitro. In a 24-well plate, 50 000 293T cells were seeded per well. One microgram of pD10/CMV-*Aipl1* was used to transfect each well along with Lipofectin and peptide6 in the ratio described above, and 1 μl of AAV-CMV-*Aipl1* (10^{11} vp/mL) was added to each well. Replicates of 12 were performed for plasmid transfection and virus infection, respectively. Transfected cells were collected 24 h later and infected cells were harvested at 48 h. The cells were lysed and the lysates pooled together. A standard western blot was performed using anti-AIPL1 antibody.

Total retinal RNA was isolated from treated and untreated *Aipl1* h/h and from wild-type mice using TRIzol reagent (Invitrogen, Paisley, UK). Reverse transcription of RNA into cDNA was performed by using the Transcriptor First Strand cDNA Synthesis Kit (Roche Diagnostics, Burgess Hill, UK). Beta-actin was amplified as an internal standard. PCR primers for beta-actin quantitative PCR were 5′- GGAGG GGGTTGAGGTGTT and 3′- TGTGCACTTTTATTGGTCT CAAG. Primers for mAIPL1 quantitative PCR were 5′-GACGCTGCTGACCTCCAT and 3′- GCGGGACAACA TAGGGTAGA. PCR was carried out for 40 cycles of 95°C (15 s), followed by 60°C (60 s).

Immunohistochemistry, morphometric analysis and immunoblotting

Wild-type eyes, treated and untreated *Aipl1* h/h eyes were harvested; a cautery mark was placed on the limbus to aid orientation of the eyes, to ensure that quantification of photoreceptors and immunostaining were performed on equivalent areas on treated and untreated eyes. The eyes were embedded directly in Optimal Cutting Temperature (OCT) medium (RA Lamb, E. Sussex, UK), frozen in isopentane which had been precooled in liquid nitrogen and were stored at −80°C. Immunofluorescence for AIPL1 and ß-PDE were performed on freshly cut, frozen retinal sections which had been serially sectioned at thickness of 9–10 μm. Cryosection slides were air-dried, post-fixed briefly in 1%PFA and incubated in blocking buffer [10% normal goat serum (Dako Ltd.), 0.1% Tween and 3% BSA in TBS] for 1 h at room temperature. A polyclonal anti-AIPL1 antibody was diluted 1:500 in blocking buffer and slides were incubated overnight at 4°C with the anti-AIPL1 antibody (30). After washes in TBS, slides were incubated with the secondary antibody, Alexa Fluor® 488 goat anti-rabbit IgG conjugate (Molecular Probes, Leiden, The Netherlands) at dilution of 1:150 in TBS for 2 h. Slides were then washed in TBS before a second overnight incubation at 4°C with ß-PDE antibody purchased from Affinity BioReagents (Neshanic Station, NJ, USA), diluted at 1:500 in blocking buffer. Following overnight incubation, slides were washed in TBS and incubated with quaternary antibody, Alexa Fluor® 546 goat anti-rabbit IgG conjugate (Molecular Probes, Leiden, The Netherlands) at dilution of 1:150 in TBS for 2 h. Slides were washed again in TBS and counterstaining of the nuclei was performed using Hoechst 33342 diluted at 1:1000. Slides were mounted in fluorescent mounting medium (Fluormount, Dako) and sections examined by fluorescent microscopy and images captured on Leica DC 500 (Zeiss, Germany) digital camera.

For morphometric analysis, retinas were taken at the final time point of ERG analysis. Cryosections were cut at different levels through the whole horizontal extension of the retina and each eye was orientated so that each section spanned over the superior and inferior retina which are the sites of injection. Freshly cut, frozen sections at thickness of 10–12 μm were stained with propidium iodide (PI) to stain photoreceptor nuclei. To standardize measurements, three sagittally orientated central sections which passed through the optic nerve head were selected for the analysis. Images were captured from each side of the optic nerve head in each section, at approximately midpoint of the distance between the optic disc and the ora serrata. Sections from matched treated and untreated eyes were imaged at the same magnification using confocal microscopy (Zeiss, LSM 510). The nuclei in the outer nuclear layer in this area were counted by a single masked observer. The photoreceptor cell count for each eye was determined by averaging the cell counts from each confocal image of the eye. To control for inter-animal variation in the rate of degeneration, a paired *t*-test was performed between the photoreceptor cell counts in the treated and untreated eyes of each animal.

For immunoblotting, equal amounts (5–10 μg) of samples (cell lysates or retinal homogenates) were separated on 9% SDS–polyacrylamide gel and transferred by electroblotted to polyvinylidene difluoride membranes (Immobilion-P, Millipore). Membranes were blocked at room temperature for an hour and incubated overnight with primary antibodies, rabbit anti-Aipl1 antibody and rabbit ß-PDE antibody (both described above) and with mouse monoclonal anti-ß-actin antibody (Sigma) for loading controls at 16°C. After washing, the membranes were then incubated with peroxidase-conjugated secondary antibodies (goat anti-rabbit IgG and goat anti-mouse IgG, horseradish peroxidase conjugated antibody, Jackson Immunoresearch) for an hour at room temperature followed by further washes and developed by ECL substrates (ECL Plus Western Blotting Detection System, GE Healthcare).

Semithin sections and transmission electron microscopy

Prior to fixation, eyes for semithin sectioning were orientated by putting a suture on the nasal aspect of the eyes. Eyes were immersion fixed in 3% glutaraldehyde and 1% paraformaldehyde buffered to pH 7.4 with 0.07 M sodium cacodylate-HCL. After a minimum of 12 h of fixation, the cornea and lens were removed. The posterior segments were then osmicated for 2 h with a 1% aqueous solution of osmium tetroxide and dehydrated through ascending alcohols (50–100%, 10 min per step). After three changes of 100% ethanol, the specimens were passed through propylene oxide (2 × 20 min) and left overnight in a 50:50 mixture of propylene oxide and araldite. Following a single change to fresh araldite (5 h with rotation), the specimens were embedded and cured for 24 h at 60°C. Using the nasal suture, the eyes were embedded sagittally so that sectioning occurred in the vertical plane and the retinal sections contained the superior and inferior retina. Semithin (0.7 μm) and ultrathin (0.07 μm) sections were cut using a Leica Ultracut S microtome fitted with an appropriate diamond knife (Diatome histoknife Jumbo or Diatome Ultrathin). Following sequential contrasting

with 1% uranyl acetate and lead citrate, the ultrathin section was analysed and photographed using a JEOL 1010 Transmission Electron Microscope operating at 80 kV. Semithin sections were stained with 1% toluidine blue and evaluated using a Leitz Diaplan microscope fitted with a Leica digital camera DC 500 for image capture.

Electroretinographic analysis

Electroretinograms (ERGs) were recorded from both eyes of *Aipl1*−/− mice ∼2 weeks following subretinal injections (∼P28) and from Aipl1 h/h mice at 4 weekly intervals following subretinal injections. All animals were dark-adapted overnight (16 h) and anaesthetized with a single intraperitoneal injection of 0.15 ml of a mixture of Domitor (1 mg/ml medetomidine hydrochloride), and ketamine (100 mg/ml), and water in the ratio 5:3:42 prior to testing. The pupils were dilated using on drop of Tropicamide 1% and phenylephrine hydrochloride 2.5%. A single drop of 2% hydroxypropylmethylcellulose was placed on each cornea to keep it moistened and mice were then placed on a heated platform. ERGs were recorded using commercially available equipment (Toennies Multiliner Vision; Jaeger/Toennies, Germany for experiments in Figs 2 and 4; Espion E2; Diagnosys LLC, Massachusetts USA for experiments in Fig. 5) after corneal contact electrodes and midline subdermal reference and ground electrodes were placed. Bandpass filter cut-off frequencies were 1 and 300 Hz. Single flash recordings were obtained at light intensities increasing from 0.1 to 5000 mcds/m^2 presented in a ganzfeld dome. Ten responses per intensity level were averaged with an interstimulus interval of 5 s (0.1, 1, 10 and 100 mcds/m^2) or five responses per intensity with a 17 s interval (1000 and 3000 mcds/m^2). Dark-adapted, rod dominated responses were elicited in the dark with 10 μs flashes of white light (1.37×10^5 cd/m^2) presented at intervals of 1 min. Light-adapted, cone responses were elicited in the presence of a 41 cd/m^2 rod-desensitizing white background with the same flashes (1.37×10^5 cd/m^2) presented at intervals of 1 Hz.

Statistical analysis

For ERG analysis, the b-wave amplitude at 1000 mcds/m^2 was used. The b-wave values (a-wave trough b-wave peak) of the treated (right) eye were paired with the untreated contralateral (left) eye to provide an internal control. This method controls for interanimal variance and test–retest variance present in rodent ERGs. For analysis of the ERG b-wave amplitudes and photoreceptor cell numbers, paired Student's *t*-tests were used to determine significance ($P < 0.05$).

SUPPLEMENTARY MATERIAL

Supplementary Material is available at *HMG* online.

ACKNOWLEDGEMENTS

We thank Drs Melanie Sohocki and Michael Dyer for providing the *Aipl1*−/− mice. M.H.T. is a Medical Research Council Clinical Training Fellow.

Conflict of Interest statement. None declared.

FUNDING

H.V.T. is supported by Fonds National Suisse de la Recherche Scientifique, Roche Research Foundation and Holcim Stiftung zur Förderung der wissenschaftlichen Fortbildung. This work was also supported by grants from the European Union (AAVEYE), the UK Department of Health, National Institute of Health Research BMRC for Ophthalmology, NIH Grant EY10581 and Foundation Fighting Blindness.

REFERENCES

1. Perrault, I., Rozet, J.M., Gerber, S., Ghazi, I., Leowski, C., Ducroq, D., Souied, E., Dufier, J.L., Munnich, A. and Kaplan, J. (1999) Leber congenital amaurosis. *Mol. Genet. Metab.*, **68**, 200–208.
2. Schuil, J., Meire, F.M. and Delleman, J.W. (1998) Mental retardation in amaurosis congenita of Leber. *Neuropediatrics*, **29**, 294–297.
3. Ali, R.R., Sarra, G.M., Stephens, C., Alwis, M.D., Bainbridge, J.W., Munro, P.M., Fauser, S., Reichel, M.B., Kinnon, C., Hunt, D.M. *et al.* (2000) Restoration of photoreceptor ultrastructure and function in retinal degeneration slow mice by gene therapy. *Nat. Genet.*, **25**, 306–310.
4. Acland, G.M., Aguirre, G.D., Ray, J., Zhang, Q., Aleman, T.S., Cideciyan, A.V., Pearce-Kelling, S.E., Anand, V., Zeng, Y., Maguire, A.M. *et al.* (2001) Gene therapy restores vision in a canine model of childhood blindness. *Nat. Genet.*, **28**, 92–95.
5. Lai, C.M., Yu, M.J., Brankov, M., Barnett, N.L., Zhou, X., Redmond, T.M., Narfstrom, K. and Rakoczy, P.E. (2004) Recombinant adeno-associated virus type 2-mediated gene delivery into the Rpe65−/− knockout mouse eye results in limited rescue. *Genet. Vaccines Ther.*, **2**, 3.
6. Smith, A.J., Schlichtenbrede, F.C., Tschernutter, M., Bainbridge, J.W., Thrasher, A.J. and Ali, R.R. (2003) AAV-mediated gene transfer slows photoreceptor loss in the RCS rat model of retinitis pigmentosa. *Mol. Ther.*, **8**, 188–195.
7. Pawlyk, B.S., Smith, A.J., Buch, P.K., Adamian, M., Hong, D.H., Sandberg, M.A., Ali, R.R. and Li, T. (2005) Gene replacement therapy rescues photoreceptor degeneration in a murine model of Leber congenital amaurosis lacking RPGRIP. *Invest Ophthalmol. Vis. Sci.*, **46**, 3039–3045.
8. Pang, J.J., Chang, B., Kumar, A., Nusinowitz, S., Noorwez, S.M., Li, J., Rani, A., Foster, T.C., Chiodo, V.A., Doyle, T. *et al.* (2006) Gene therapy restores vision-dependent behavior as well as retinal structure and function in a mouse model of RPE65 Leber congenital amaurosis. *Mol. Ther.*, **13**, 565–572.
9. Acland, G.M., Aguirre, G.D., Bennett, J., Aleman, T.S., Cideciyan, A.V., Bennicelli, J., Dejneka, N.S., Pearce-Kelling, S.E., Maguire, A.M., Palczewski, K. *et al.* (2005) Long-term restoration of rod and cone vision by single dose rAAV-mediated gene transfer to the retina in a canine model of childhood blindness. *Mol. Ther.*, **12**, 1072–1082.
10. Tschernutter, M., Schlichtenbrede, F.C., Howe, S., Balaggan, K.S., Munro, P.M., Bainbridge, J.W., Thrasher, A.J., Smith, A.J. and Ali, R.R. (2005) Long-term preservation of retinal function in the RCS rat model of retinitis pigmentosa following lentivirus-mediated gene therapy. *Gene Ther.*, **12**, 694–701.
11. Batten, M.L., Imanishi, Y., Tu, D.C., Doan, T., Zhu, L., Pang, J., Glushakova, L., Moise, A.R., Baehr, W., Van Gelder, R.N. *et al.* (2005) Pharmacological and rAAV gene therapy rescue of visual functions in a blind mouse model of Leber congenital amaurosis. *PLoS. Med.*, **2**, e333.
12. Bainbridge, J.W., Smith, A.J., Barker, S.S., Robbie, S., Henderson, R., Balaggan, K., Viswanathan, A., Holder, G.E., Stockman, A., Tyler, N. *et al.* (2008) Effect of gene therapy on visual function in Leber's congenital amaurosis. *N. Engl. J. Med.*, **358**, 2231–2239.
13. Maguire, A.M., Simonelli, F., Pierce, E.A., Pugh, E.N. Jr, Mingozzi, F., Bennicelli, J., Banfi, S., Marshall, K.A., Testa, F., Surace, E.M. *et al.* (2008) Safety and efficacy of gene transfer for Leber's congenital amaurosis. *N. Engl. J. Med.*, **358**, 2240–2248.
14. Cideciyan, A.V., Aleman, T.S., Boye, S.L., Schwartz, S.B., Kaushal, S., Roman, A.J., Pang, J.J., Sumaroka, A., Windsor, E.A., Wilson, J.M. *et al.* (2008) Human gene therapy for RPE65 isomerase deficiency activates the

retinoid cycle of vision but with slow rod kinetics. *Proc. Natl Acad. Sci. USA*, **105**, 15112–15117.
15. Ali, R.R., Reichel, M.B., Thrasher, A.J., Levinsky, R.J., Kinnon, C., Kanuga, N., Hunt, D.M. and Bhattacharya, S.S. (1996) Gene transfer into the mouse retina mediated by an adeno-associated viral vector. *Hum. Mol. Genet.*, **5**, 591–594.
16. Rabinowitz, J.E. and Samulski, R.J. (2000) Building a better vector: the manipulation of AAV virions. *Virology*, **278**, 301–308.
17. Natkunarajah, M., Trittibach, P., McIntosh, J., Duran, Y., Barker, S.E., Smith, A.J., Nathwani, A.C. and Ali, R.R. (2007) Assessment of ocular transduction using single-stranded and self-complementary recombinant adeno-associated virus serotype 2/8. *Gene Ther.*, **15**, 463–467.
18. Schlichtenbrede, F.C., da Cruz, L., Stephens, C., Smith, A.J., Georgiadis, A., Thrasher, A.J., Bainbridge, J.W., Seeliger, M.W. and Ali, R.R. (2003) Long-term evaluation of retinal function in Prph2Rd2/Rd2 mice following AAV-mediated gene replacement therapy. *J. Gene Med.*, **5**, 757–764.
19. Bennett, J., Tanabe, T., Sun, D., Zeng, Y., Kjeldbye, H., Gouras, P. and Maguire, A.M. (1996) Photoreceptor cell rescue in retinal degeneration (rd) mice by in vivo gene therapy. *Nat. Med.*, **2**, 649–654.
20. Jomary, C., Vincent, K.A., Grist, J., Neal, M.J. and Jones, S.E. (1997) Rescue of photoreceptor function by AAV-mediated gene transfer in a mouse model of inherited retinal degeneration. *Gene Ther.*, **4**, 683–690.
21. Takahashi, M., Miyoshi, H., Verma, I.M. and Gage, F.H. (1999) Rescue from photoreceptor degeneration in the rd mouse by human immunodeficiency virus vector-mediated gene transfer. *J. Virol.*, **73**, 7812–7816.
22. Kumar-Singh, R. and Farber, D.B. (1998) Encapsidated adenovirus mini-chromosome-mediated delivery of genes to the retina: application to the rescue of photoreceptor degeneration. *Hum. Mol. Genet.*, **7**, 1893–1900.
23. Pang, J.J., Boye, S.L., Kumar, A., Dinculescu, A., Deng, W., Li, J., Li, Q., Rani, A., Foster, T.C., Chang, B. *et al.* (2008) AAV-mediated gene therapy for retinal degeneration in the rd10 mouse containing a recessive PDEbeta mutation. *Invest Ophthalmol. Vis. Sci.*, **49**, 4278–4283.
24. Van der, S.J., Chapple, J.P., Clark, B.J., Luthert, P.J., Sethi, C.S. and Cheetham, M.E. (2002) The Leber congenital amaurosis gene product AIPL1 is localized exclusively in rod photoreceptors of the adult human retina. *Hum. Mol. Genet.*, **11**, 823–831.
25. Chapple, J.P., Grayson, C., Hardcastle, A.J., Saliba, R.S., Van der Spuy, J. and Cheetham, M.E. (2001) Unfolding retinal dystrophies: a role for molecular chaperones? *Trends Mol. Med.*, **7**, 414–421.
26. Petrulis, J.R. and Perdew, G.H. (2002) The role of chaperone proteins in the aryl hydrocarbon receptor core complex. *Chem. Biol. Interact.*, **141**, 25–40.
27. Sohocki, M.M., Perrault, I., Leroy, B.P., Payne, A.M., Dharmaraj, S., Bhattacharya, S.S., Kaplan, J., Maumenee, I.H., Koenekoop, R., Meire, F.M. *et al.* (2000) Prevalence of AIPL1 mutations in inherited retinal degenerative disease. *Mol. Genet. Metab.*, **70**, 142–150.
28. Dharmaraj, S., Leroy, B.P., Sohocki, M.M., Koenekoop, R.K., Perrault, I., Anwar, K., Khaliq, S., Devi, R.S., Birch, D.G., De Pool, E. *et al.* (2004) The phenotype of Leber congenital amaurosis in patients with AIPL1 mutations. *Arch. Ophthalmol.*, **122**, 1029–1037.
29. Ramamurthy, V., Niemi, G.A., Reh, T.A. and Hurley, J.B. (2004) Leber congenital amaurosis linked to AIPL1: a mouse model reveals destabilization of cGMP phosphodiesterase. *Proc. Natl Acad. Sci. USA*, **101**, 13897–13902.
30. Liu, X., Bulgakov, O.V., Wen, X.H., Woodruff, M.L., Pawlyk, B., Yang, J., Fain, G.L., Sandberg, M.A., Makino, C.L. and Li, T. (2004) AIPL1, the protein that is defective in Leber congenital amaurosis, is essential for the biosynthesis of retinal rod cGMP phosphodiesterase. *Proc. Natl Acad. Sci. USA*, **101**, 13903–13908.
31. Makino, C.L., Wen, X.H., Michaud, N., Peshenko, I.V., Pawlyk, B., Brush, R.S., Soloviev, M., Liu, X., Woodruff, M.L., Calvert, P.D. *et al.* (2006) Effects of low AIPL1 expression on phototransduction in rods. *Invest Ophthalmol. Vis. Sci.*, **47**, 2185–2194.
32. Akey, D.T., Zhu, X., Dyer, M., Li, A., Sorensen, A., Blackshaw, S., Fukuda-Kamitani, T., Daiger, S.P., Craft, C.M., Kamitani, T. and Sohocki, M.M. (2002) The inherited blindness associated protein AIPL1 interacts with the cell cycle regulator protein NUB1. *Hum. Mol. Genet.*, **11**, 2723–2733.
33. Farber, D.B. (1995) From mice to men: the cyclic GMP phosphodiesterase gene in vision and disease. The Proctor Lecture. *Invest Ophthalmol. Vis. Sci.*, **36**, 263–275.
34. Semple-Rowland, S.L., Lee, N.R., Van Hooser, J.P., Palczewski, K. and Baehr, W. (1998) A null mutation in the photoreceptor guanylate cyclase gene causes the retinal degeneration chicken phenotype. *Proc. Natl. Acad. Sci. USA*, **95**, 1271–1276.
35. Perrault, I., Rozet, J.M., Calvas, P., Gerber, S., Camuzat, A., Dollfus, H., Chatelin, S., Souied, E., Ghazi, I., Leowski, C. *et al.* (1996) Retinal-specific guanylate cyclase gene mutations in Leber's congenital amaurosis. *Nat. Genet.*, **14**, 461–464.
36. Allocca, M., Mussolino, C., Garcia-Hoyos, M., Sanges, D., Iodice, C., Petrillo, M., Vandenberghe, L.H., Wilson, J.M., Marigo, V., Surace, E.M. and Auricchio, A. (2007) Novel adeno-associated virus serotypes efficiently transduce murine photoreceptors. *J. Virol.*, **81**, 11372–11380.
37. Ramamurthy, V., Roberts, M., van den Akker, F., Niemi, G., Reh, T.A. and Hurley, J.B. (2003) AIPL1, a protein implicated in Leber's congenital amaurosis, interacts with and aids in processing of farnesylated proteins. *Proc. Natl Acad. Sci. USA*, **100**, 12630–12635.
38. Van der Spuy, J. and Cheetham, M.E. (2004) The Leber congenital amaurosis protein AIPL1 modulates the nuclear translocation of NUB1 and suppresses inclusion formation by NUB1 fragments. *J. Biol. Chem.*, **279**, 48038–48047.
39. Zhang, X., De Alwis, M., Hart, S.L., Fitzke, F.W., Inglis, S.C., Boursnell, M.E., Levinsky, R.J., Kinnon, C., Ali, R.R. and Thrasher, A.J. (1999) High-titer recombinant adeno-associated virus production from replicating amplicons and herpes vectors deleted for glycoprotein H. *Hum. Gene Ther.*, **10**, 2527–2537.
40. Nathwani, A.C., Gray, J.T., McIntosh, J., Ng, C.Y., Zhou, J., Spence, Y., Cochrane, M., Gray, E., Tuddenham, E.G. and Davidoff, A.M. (2007) Safe and efficient transduction of the liver after peripheral vein infusion of self-complementary AAV vector results in stable therapeutic expression of human FIX in nonhuman primates. *Blood*, **109**, 1414–1421.

Human Molecular Genetics, 2010, Vol. 19, No. 4 **735**
doi:10.1093/hmg/ddp540

CORRIGENDUM

Gene therapy for retinitis pigmentosa and Leber congenital amaurosis caused by defects in *AIPL1*: effective rescue of mouse models of partial and complete Aipl1 deficiency using AAV2/2 and AAV2/8 vectors

Mei Hong Tan, Alexander J. Smith, Basil Pawlyk, Xiaoyun Xu, Xiaoqing Liu, James B. Bainbridge, Mark Basche, Jenny McIntosh, Hoai Viet Tran, Amit Nathwani, Tiansen Li and Robin R. Ali

Human Molecular Genetics 2009 **18**:12; pp. 2099–2114; doi:10.1093/hmg/ddp133

The Authors regret that there was an error in the Copyright status of paper '10.1093/hmg/ddp133'. The article is now freely available online under the Oxford Open model and the copyright line should have read: